

1  
2 **ORIGIN OF THREE RELATED MOVEMENT GENE MODULES IN**  
3 **PLANT VIRUSES: EVOLUTIONARY RADIATIONS OF BENYVIRUS-**  
4 **LIKE RNA REPLICONS**  
5

6  
7  
8  
9 Sergey Y. Morozov<sup>1,2,\*</sup>, and Andrey G. Solovyev<sup>1,2,3</sup>

10  
11  
12 <sup>1</sup> A. N. Belozersky Institute of Physico-Chemical Biology, Moscow State University,  
13 Moscow, Russia;

14 <sup>2</sup> Department of Virology, Biological Faculty, Moscow State University, Moscow, Russia;

15 <sup>3</sup> Sechenov First Moscow State Medical University, Institute of Molecular Medicine,  
16 Moscow, Russia

17  
18  
19  
20  
21 \* Correspondence: Sergey Morozov, [morozov@belozersky.msu.ru](mailto:morozov@belozersky.msu.ru)  
22  
23  
24  
25  
26  
27  
28  
29  
30  
31  
32  
33  
34  
35  
36  
37  
38  
39  
40

41 **ABSTRACT**

42

43 Previous studies have shown that the RNA genomes of some plant viruses encode two related  
44 genetic modules required for the virus movement over host body, containing 2 or 3 genes and  
45 named as triple gene block (TGB) and binary movement block (BMB). In this paper, we  
46 revealed a novel related movement gene module, called Tetra-Cistron Movement Block  
47 (TCMB). It was found to be encoded by virus-like transcriptome assemblies of moss  
48 *Dicranum scoparium* and Antarctic flowering plant *Colobanthus quitensis*. These TCMBs are  
49 encoded by second RNA components of the putative two-component viruses related to plant  
50 benyviruses. First, like RNA-2 of benyviruses, TCMB RNA-2 contains the 5'-terminal coat  
51 protein gene. Second, general organization of TCMB is very similar to TGB: it includes RNA  
52 helicase gene which is followed by two small overlapping cistrons encoding hydrophobic  
53 proteins with a distant sequence similarity to TGB2 and TGB3 genes. However, TCMB  
54 includes also forth 5'-terminal gene coding for protein with an obvious similarity to double-  
55 stranded RNA-binding proteins belonging to the DSRM\_AtDRB-like superfamily. Finally,  
56 we suggest the proposed involvement of replicative beny-like helicases in evolution of the  
57 BMB and TCMB movement genetic modules.

58

59

60 **Keywords:** RNA genome, plant virus, movement gene module, benyviruses, evolution, RNA  
61 helicase, plants

62

63

64

65

66

67

68

69

70

71

72

73

74

## 75 INTRODUCTION

76 All triple gene block (TGB)-containing viruses are represented by a large variety of  
77 plant RNA viruses within the orders *Martellivirales* (family *Virgaviridae*), *Tymovirales*  
78 (families *Alphaflexiviridae* and *Betaflexiviridae*) and *Hepelivirales* (family *Benyviridae*).  
79 They have a positive-sense, single-stranded genome consisting of one to four RNA segments  
80 (Morozov and Solovyev, 2003; Verchot-Lubicz et al., 2010; Koonin et al., 2020). The TGB-  
81 encoded movement proteins, referred to as TGB1, TGB2 and TGB3, perform directed  
82 transport of viral genomes to and through plasmodesmata (PD) into adjacent non-infected  
83 cells. TGB1 contains protein domain of RNA helicase of superfamily 1 (SF1), whereas TGB2  
84 and TGB3 are the small membrane-associated proteins and contain highly hydrophobic  
85 amino acid segments (Verchot-Lubicz et al., 2010). Recently, binary movement block  
86 (BMB), which is related to TGB, was found in kitaviruses (family *Kitaviridae*, order  
87 *Martellivirales*). This gene module includes only two genes (BMB1 and BMB2). Although  
88 pairs of BMB1/TGB1 and BMB2/TGB2 proteins are quite similar in structural, functional  
89 and phylogenetic aspects (Morozov and Solovyev, 2015, 2020; Solovyev and Morozov,  
90 2017; Lazareva et al., 2017; 2021), BMB gene module lacks analog of TGB3. Importantly,  
91 recent data showed that some viruses from genera *Potexvirus* and *Carlavirus* encode no  
92 TGB3 proteins, despite the fact that TGB1 and TGB2 proteins of these viruses are  
93 significantly similar to those of potexvirus-like TGBs (Morozov and Solovyev, 2015). These  
94 observations support the hypothesis that the TGB3 gene could be a less essential component  
95 (an accessory cistron) of transport gene module. Conceivably, TGB3 could be evolved as an  
96 additional cistron if BMB was the first transport module of this type appeared in virus  
97 genomes or, alternatively, could be eliminated during evolution of earliest TGB-related  
98 movement modules (Morozov and Solovyev, 2015, 2020; Solovyev and Morozov, 2017).  
99 Taking into account these considerations, identification of new TGB/BMB-like gene modules  
100 in lower land plants could shed a new light on the early steps of TGB/BMB evolution. So far,  
101 only a single TGB-containing virus-like RNA assembly has been revealed in non-seed plants,  
102 namely, bird's-nest fern *Asplenium nidus*. This fern virus shows gene arrangements and  
103 sequence similarities indicating its close relatedness to benyviruses (Morozov and Solovyev,  
104 2015).

105 In our recent paper, we draw attention to partial transcriptome assemblies in the  
106 Antarctic flowering plant *Colobanthus quitensis*, where a probable evolutionary early variant  
107 of TGB was found (Cq-TGB) (Solovyev and Morozov, 2017). Importantly, the Cq-TGB1  
108 protein sequence is more similar to BMB1 in comparison with TGB1 proteins (Fig. 1).

109 Moreover, the central hydrophilic region of Cq-TGB3 protein located between two  
110 transmembrane sequence segments shows clear amino acid sequence similarity to the Cq-  
111 TGB2 protein and exhibits conservation of most amino acid residues invariant in other TGB2  
112 proteins (Solovyev and Morozov, 2017). These data suggest that Cq-TGB could arise from a  
113 BMB-like module by duplication of hydrophobic protein gene. Importantly, the Antarctica  
114 coast flora was isolated from the rest of the world for approximately 20 million years  
115 (Cantrill and Poole, 2013). This fact provided a reasonable basis for considering Cq-TGB as  
116 one of the ancient movement gene modules and further prompted us to search available  
117 sequence data to find more viral gene blocks related to TGB/BMB modules in transcriptomes  
118 of non-seed plants and extant land plants.

119 In this paper, we reported new virus-like RNA assemblies (VLRAs) in the NCBI TSA  
120 and SRA databases and identified a novel plant virus movement gene module in the  
121 transcriptome samples of two wild plant species. This gene module could be classified as  
122 structurally and evolutionary related to BMB and TGB. Additionally, we presented new data  
123 supporting an idea that the movement gene modules related to TGB could initially originate  
124 in the benyvirus-like replicons.

## 125 **NOVEL MOVEMENT GENE MODULE IN THE VIRUS-RELATED PLANT** 126 **TRANSCRIPTOMES: TETRA-CISTRON MOVEMENT BLOCK**

127 We undertook a systematic analysis of RNA-seq datasets from Viridiplantae available  
128 in the NCBI open-access TSA and SRA in the end of November, 2021. Our TBLASTn  
129 search of plant TSA data collection, using Cq-TGB encoded helicase (accession  
130 GCIB01126289) as a query, resulted in the identification of a new partial VLRA (accession  
131 HANF01089872) in moss *Dicranum scoparium* (family *Dicranaceae*, order Dicranales)  
132 encoding protein with obvious similarity to Cq-TGB1 (Fig. 1). Using transcriptome  
133 sequencing data for the *D. scoparium* SRA experiment (ERX3824048), we further assembled  
134 a nearly full-length sequence of the contig (Ds-VLRA2) comprised 3,996 nt excluding the  
135 poly(A) tail. The open reading frame (ORF) prediction at ExPASy (ESTscan) showed that the  
136 contig contains six ORFs flanked by a 5' untranslated region (5' UTR, at least 183 nt) and a  
137 3' UTR (165 nt) (Fig 2A). The resulting *D. scoparium* VLRA exhibits a gene content and  
138 arrangement quite similar to that in RNA 2 of benyviruses (Fig. 2B) (Saito et al., 1996).  
139 Indeed, this RNA encodes the 5'-terminal coat protein (CP) gene (ORF1) and TGB-like  
140 module (Fig. 2A). Although the CP of Ds-VLRA2 (220 aa in length) has only marginal  
141 amino acid similarity with the members of genus *Benyvus*, it shows obvious similarity to

142 other tobamovirus-like CPs, namely, the tobacco rattle virus CP (genus *Tobravirus*; family  
143 *Virgaviridae*) (ABE27877, 31% identity, E-value 1e-11), and the pea early-browning virus  
144 CP (genus *Tobravirus*; family *Virgaviridae*) (CAA07067, 29% identity, E-value 2e-11).

145 The ORF2 and ORF3 of Ds-VLRA2 encode proteins of 301 aa and 120 aa residues in  
146 length, respectively (Fig.2A). BLASTn and BLASTx analyses showed that ORF2 protein has  
147 no significant sequence homology with known virus polypeptides (data not shown). The  
148 NCBI Conserved Domain Database (CDD) analysis identified that the ORF2 protein could  
149 contain a possible domain related to the SMC superfamily (Accession No. cl34174, E-value  
150 6.56e-03). The SMC (structural maintenance of chromosomes) domain is found in the  
151 proteins that bind DNA and act in organizing and segregating chromosomes (Lehmann,  
152 2005). Additional protein domain analyses using ExPASy (ProtScale) software predicted a  
153 coiled-coil motif located at amino acid positions 136–185 and two highly hydrophobic  
154 sequences positioned at residues 45–63 and 279-299 in ORF2 protein (Fig. 3).

155 The NCBI CDD analysis also identified a possible domain in the ORF3 protein,  
156 corresponding to the DSRM\_AtDRB-like superfamily (Accession No. cl00054, E-value 1.6e-  
157 03). Therefore, the Ds-VLRA2 ORF3 protein was named viral DRB (vDRB). The DSRM  
158 protein domain superfamily is a well-known protein structural motif of 65-70 aa in length that  
159 adopts an alpha-beta-beta-beta-alpha fold and binds double-stranded RNAs (dsRNAs) of  
160 various origin and structure. This family includes a group of *Arabidopsis thaliana* double-  
161 stranded RNA-binding proteins termed AtDRB1-AtDRB5. Members of this group usually  
162 contain two DSRM domains. They bind dsRNA and are involved in RNA-mediated silencing  
163 (Han et al., 2004; Eamens et al., 2012) and/or dsRNA-triggered immunity against viruses  
164 (Fátyol et al., 2020). The vDRB protein encoded by Ds-VLRA2 contains a single DSRM  
165 showing conservation of key residues specific for DSRM\_AtDRB-like proteins (Fig. 4).  
166 Interestingly, AtDRB-like proteins are encoded not only by flowering plants but also  
167 representatives of lower vascular plants (Lycopodiopsida), mosses (Bryophyta) and  
168 liverworts (Marchantiophyta). Moreover, these proteins can be revealed in present-day  
169 Charophyte algae (members of Zygnemophyceae and Charophyceae families), which are  
170 assumed to be the closest relatives of land plants descendent of the organisms that took part  
171 in initial colonization of terrestrial habitats (Fig. 4). Importantly, the Ds-VLRA2 vDRB  
172 protein, unlike AtDRB1-AtDRB5, contains a hydrophobic transmembrane segment at the N-  
173 terminus (Fig. 5).

174 The ORF4 in Ds-VLRA2 overlaps the ORF3 by 60 nucleotides (Fig. 2A) and encodes  
175 protein of 361 residues containing motifs characteristic for helicases of SF1 superfamily and

176 showing obvious similarity to BMB1 helicases (Fig. 1). ORF4 is followed by overlapping  
177 ORF5 and ORF6 (Fig. 2A), which code for small hydrophobic proteins with two putative  
178 transmembrane domains and central hydrophilic region related to TGB2/BMB2 proteins (Fig.  
179 6). Protein sequence similarity of the encoded proteins and general organization of the gene  
180 block represented by ORFs 4-6 of Ds-VLRA2 resembles TGB and related Cq-TGB-like  
181 module (accession GCIB01126289).

182 Taking into account the similarity of Ds-VLRA2 TGB and Cq-TGB, we further  
183 analyzed whether the previously assembled *C. quitensis* TGB-containing VLRA was  
184 incomplete and could be extended into the 5'-terminus direction. Our *de novo* assembly of  
185 transcriptome sequencing data for *C. quitensis* SRA experiment (SRX814890) resulted in the  
186 probable full-length contig (Cq-VLRA2) of 4,718 nt in length excluding the poly(A) tail.  
187 The resulting sequence was confirmed using incomplete contigs from TSA database  
188 (GCIB01147888, GCIB01142942, GCIB01133924 and GCIB01126289). The ORF  
189 prediction at ExPASy showed that this contig contains seven ORFs flanked by a 5'-  
190 untranslated region (5'-UTR, at least 259 nt) and a 3'-UTR (213 nt). The 5'-terminal ORF1  
191 encodes a capsid protein (164 aa in length) (Fig 2A) showing similarity to the wheat stripe  
192 mosaic virus CP (genus *Benyvirus*) (YP009553316, 27% identity, E-value 1e-04), and the  
193 sorghum chlorotic spot virus CP (genus *Furovirus*; family *Virgaviridae*) (NP659022, 29%  
194 identity, E-value 3e-04). The next ORF2 represents read-through domain of CP fusion protein  
195 as it was reported for benyviruses (Fig. 2B) (Saito et al., 1996). Among three described types  
196 of read-through nucleotide signatures, ORFs1/2 contain the type I motif containing a UAG  
197 codon, which is followed by the consensus motif CARYYA (where R is a purine and Y is a  
198 pyrimidine). This mechanism of translation is also used in tobamovirus replicase genes (Firth  
199 and Brierley, 2012; Miras et al., 2017).

200 ORF2 is followed by an intergenic region of 73 nucleotides in length and an ORF3,  
201 which codes for a small protein with the charged N-terminal half and cysteine-rich C-  
202 terminal region (Fig. 2A, Fig. 7). This cysteine-rich protein (CRP) shows no sequence  
203 similarity to the RNA2-encoded benyvirus CRP (Fig. 2B), and its cysteine-rich region is  
204 marginally similar to double zinc finger motif-containing module of FYVE domain involved  
205 in mRNA transport to endosomes (Pohlmann et al., 2015).

206 The NCBI BLAST analysis showed that Cq-VLRA2 ORF4 protein is quite similar to  
207 Ds-ORF3 (vDRB) protein and contains single DSRM with signatures specific for  
208 DSRM\_AtDRB-like proteins (Fig. 4) and the N-terminal hydrophobic segment (Fig. 5). Cq-  
209 ORF4 is followed by an overlapping ORF5 encoding protein of 355 amino acids in length

210 (Fig. 2A). The Cq-ORF5 protein (earlier named Cq-TGB1, see above) possesses motifs  
211 characteristic for helicases of SF1 superfamily and shows significant similarity to Ds-ORF4  
212 protein (Ds-TGB1) and BMB1 helicases (Fig. 1). Like Ds-VLRA2, Cq-ORF4 is followed by  
213 overlapping ORFs 5 and 6 (Fig. 2) encoding small hydrophobic proteins with two putative  
214 transmembrane domains and central hydrophilic region related to Ds-ORF5/6 proteins (Fig.  
215 6).

216 A general view on the organization of Ds-VLRA2 and Cq-VLRA2 strongly suggests  
217 two conclusions: 1) Both virus-like RNAs have considerable similarity to the benyvirus  
218 TGB-containing RNA2. Indeed, RNA2 of the type benyvirus Beet necrotic yellow vein virus  
219 (BNYVV) has six ORFs, namely, the CP gene terminated by a leaky stop codon, the CP read-  
220 through protein gene, the TGB and the cistron coding for a cysteine-rich protein having a  
221 silencing suppressor activity (Fig. 2B) (Saito et al., 1996; Chiba et al., 2013); 2) These RNAs  
222 include a conserved module of four overlapping genes, which is proposed to be named  
223 “Tetra-Cistron Movement Block” (TCMB). In comparison with the TGB and BMB modules,  
224 TCMB includes an additional 5'-terminal ORF, which overlaps the downstream gene and  
225 codes for the vDRB protein with a novel, previously undescribed for virus-encoded proteins,  
226 dsRNA-binding activity. Importantly, the cellular DRBs were shown to be incorporated into  
227 virus-specific replication membrane compartments (Barton et al., 2017; Incarbone et al.,  
228 2021), the structures often located at the PD orifice and involved in virus cell-to-cell  
229 movement (Tilsner et al., 2013). Similarly, the related hydrophobic vDRB proteins could be  
230 proposed to work in concert with other TCMB proteins to take part in viral dsRNA delivery  
231 to and/or retaining in PD-associated ER membrane-derived replicative compartments (Tilsner  
232 et al., 2013; Lazareva et al., 2021) and, thus, participate in virus cell-to-cell movement.

## 233 **PROPOSED GENERAL ORGANIZATION OF TCMB-CONTAINING PLANT** 234 **VIRUS GENOMES**

235 Assuming similarity of Ds-VLRA2 and Cq-VLRA2 to benyvirus RNA2 (Fig. 2) in  
236 gene organization, we performed search of the NCBI *Dicranum scoparium* TSA database in  
237 an attempt to find Ds-RNA1 expecting to code for virus replicase as in the case of BNYVV.  
238 As an initial query, we used 150 amino acid-long segment of BNYVV replicase (GDD  
239 domain). BLAST search revealed a single TSA contig (HANF01090670) of 305 nucleotides  
240 in length which codes for a protein segment containing a GDD motif typical for RNA-  
241 dependent RNA polymerase (RdRp) domain and having more than 60% protein identity to  
242 BNYVV replicase protein (data not shown). To assemble the expected Ds-RNA1,

243 transcriptome sequencing data for *D. scoparium* SRA experiment ERX3824048 linked to the  
244 TSA project were used. The assembled full-length sequence of the contig comprised 6,624 nt,  
245 excluding the poly(A) tail. ORF prediction showed that the contig contains a single cistron  
246 encoding viral replicase flanked by a 5'-UTR (at least 78 nt) and a 3' UTR (237 nt) (Fig. 8A).  
247 Importantly, pairwise BLASTN analysis of the 3'-untranslated regions from Ds-VLRA1 and  
248 Ds-VLRA2 indicated a significant degree of sequence conservation among them and strongly  
249 suggested that both moss VLRAAs are indeed the two components of a single virus genome  
250 (Fig. 8B).

251 ORF1 protein of Ds-VLRA1 contains four conserved domains: a viral  
252 methyltransferase domain (MTR, pfam01660, amino acid positions 440–625, E-value 2.58e-  
253 06); a viral helicase 1 domain (HEL, pfam01443, amino acid positions 939-1179, E-value  
254 4.70-22); papain-like proteinase domain (PROT, pfam05415, positions 1333-1408, E-value  
255 6.97-06), and RdRp core motif (pfam00978, amino acid positions 1698–2045, E-value 2.42e-  
256 14) (Fig. 8A). The MTR domain is known to be conserved in a wide range of single-stranded  
257 RNA viruses, including orders *Martellivirales*, *Tymovirales* and *Hepelivirales* (Rozanov et  
258 al., 1992). All replicases in the members of these orders also encode HEL and RdRp domains  
259 containing typical motifs (Koonin and Dolja, 1993) conserved also in the ORF1 protein of  
260 Ds-VLRA1. Although the protease domain is not common for the above-mentioned  
261 replicases, Ds-VLRA1 encodes a protein domain with similarity to benyvirus protease (Fig.  
262 8A), which is conserved in most benyviruses and required to produce mature replicase  
263 proteins by proteolytic self-cleavage (Rodamilans et al., 2018).

264 We further used encoded amino acid and nucleotide sequences of Ds-VLRA1 as  
265 queries for searches of *C. quitensis* SRA data (SRX814890) in order to assemble a Cq-RNA1  
266 complete nucleotide sequence. However, only a rather short nucleotide sequence encoding a  
267 part of RdRp domain (including the GDD signature), which showed significant similarity to  
268 Ds-VLRA1 protein and moderate similarity to benyvirus replicases, has been assembled (Fig.  
269 9).

270

## 271 **CLUES TO THE POSSIBLE ORIGINATION OF HELICASES ENCODED BY BMB** 272 **AND TCMB**

273 An important clue to the pathways of evolutionary origin of TGB, BMB and TCMB,  
274 to our mind, is provided by phylogenetic analysis of their encoded helicases. Evidently, BMB  
275 and TCMB helicases form a common branch which is closer to benyvirus TGB helicases and  
276 less similar to potex- and hordei-like TGB helicases (Fig. 1). Moreover, BMB and TCMB



277 helicases show more sequence identity to beny-like replication helicases than to potex- and  
278 hordei-like TGB helicases (Morozov and Solovyev, 2015). Therefore, it can be suggested that  
279 a starting event in the evolutionary emergence of BMB- and TCMB could be duplication and  
280 autonomization of the replicative helicase domain occurred due to template switching during  
281 the virus genome replication along with probable non-replicative joining of RNA fragments  
282 (Bujarsky, 2013). Such RNA-RNA recombination likely resulted in the formation of the  
283 earliest monopartite and/or multipartite beny-like replicons with an autonomized copy of SF1  
284 helicase. Recombination-dependent scenarios for evolutionary radiation have been also  
285 proposed for viruses of the family *Hepeviridae* (Kelly et al., 2016), which, together with  
286 benyviruses and tetraviruses (Dorrington et al., 2020), comprise the order *Hepelivirales*  
287 (Koonin et al., 2020). Taking into account the fact that the currently revealed TCMB-  
288 containing viruses infect primitive land plant (moss) (this paper) or the geographically long-  
289 term isolated flowering plant *C. quitensis* (Solovyev and Morozov, 2017), TCMB might be  
290 considered as an evolutionary old movement gene module originated in benyvirus-like  
291 replicons.

292

## 293 **ORIGINATION OF HYDROPHOBIC PROTEIN GENES IN MOVEMENT**

### 294 **GENETIC MODULES**

295 As it was suggested above, possible starting event in evolution of BMB- and TCMB-  
296 containing viruses was the formation of the beny-like replicons with an autonomized  
297 (duplicated) copy of beny-like SF1 replicative helicase. However, phenomenon of origination  
298 and acquisition of hydrophobic protein genes in different types of movement gene modules is  
299 generally obscure (Morozov and Solovyev, 2015; 2020). In this study, we found that among  
300 monopartite plant beny-like viruses, in addition to BMB-containing replicons, many VLRA  
301 and viruses contain one or two small ORFs, which are located downstream of the replicase  
302 gene and encode small “orphan” proteins with one or two hydrophobic segments (Fig. 9 and  
303 Fig. 10) (Solovyev and Morozov, 2017).

304 We hypothesize that these hydrophobic “orphan” protein ORFs have originated due to  
305 recombination of viral RNAs with host transcripts containing *de novo* emerged ORFs.  
306 Indeed, it was proposed that novel eukaryotic “orphan” protein-coding genes can arise *de*  
307 *novo* in non-coding sequences, which, thus, may serve as a continuous reservoir of variable  
308 novel polypeptides serving as a raw material for natural selection (Vakirlis et al., 2020).  
309 Moreover, evolution of non-coding thymine-rich sequences can result in preferable  
310 emergence of ORFs encoding proteins with hydrophobic domains (Vakirlis et al., 2020;

311 Fesenko et al., 2021). These findings allowed our colleagues to propose a novel evolutionary  
312 model suggesting that ORFs for small membrane-bound polypeptides emerging *de novo* in  
313 basal land plants could be a preferential subject of adaptive evolution because of escape of  
314 their encoded proteins from degradation or other deleterious interactions in the membrane  
315 environment (Fesenko et al., 2021). Therefore, viruses similar to the above-mentioned  
316 monopartite beny-like replicons, which might be produced through recombination with  
317 mRNAs carrying such ORFs for membrane polypeptides, can be proposed to serve as sources  
318 of ancestral membrane protein genes for recombination-dependent evolution TCMB- and  
319 BMB-like genetic modules and also some other movement genetic modules described for  
320 plant viruses (Morozov and Solovyev, 2020).

321

## 322 **EVOLUTIONARY RADIATION OF BENYVIRUS-LIKE RNA REPLICONS**

323 Assuming the proposed involvement of replicative beny-like helicase in evolution of  
324 the above-mentioned movement genetic modules, it is tempting to speculate on the global  
325 evolution of beny-like replication proteins. Generally, a phylogenetic tree of selected beny-  
326 like RdRp domains (Fig. 9) showed three main branches including (i) a basal branch  
327 composed of closely related RNA viruses from fresh-water species of algal genus *Chara*  
328 *found in Australia and Canada* (Gibbs et al., 2011; Vlok et al., 2019); (ii) a branch of  
329 benyviruses (Niehl et al., 2020), plant bipartite viruses with TCMB (this study) and related  
330 monopartite plant beny-like viruses and VLRA; (iii) a mixed branch including fungal and  
331 arthropod viruses, as well as VLRA from red algae. Indeed, recent advances in sequencing  
332 benyvirus-like RNA replicons revealed their multiple hosts not only in plants but also among  
333 arthropods (particularly, *Bemisia tabaci* beny-like virus 6 - MW256699; *Bemisia tabaci* beny-  
334 like virus 4 - MW256697; Hubei Beny-like virus 1 - MK231108; *Diabrotica undecimpunctata*  
335 virus 2 - MN646771) and fungi (particularly, *Erysiphe necator* associated beny-like virus 1 -  
336 MN617775; *Rhizoctonia solani* beny-like virus 1 - MK507778; *Sclerotium rolfsii* beny-like  
337 virus 1 - MH766487) (Fig. 9) (Shi et al., 2016; Zhu et al., 2018; Picarelli et al., 2019; Gilbert  
338 et al., 2019; Liu et al., 2020).

339 Significantly, among monopartite Viridiplantae viruses, the beny-like replicase is  
340 encoded by two viruses with an unusual gene organization, namely, beny-like *Chara* virus  
341 (Vlok et al., 2019) and goji berry chlorosis virus (GBCV) (Kwon et al., 2018). It is known  
342 that charophyte algae are considered as the ancestors of land plants, and *Chara* viruses may  
343 be evolutionarily related to ancestor virus species that infected first plants colonizing  
344 terrestrial habitats (Vlok et al., 2019). Interestingly, beny-like *Chara* viruses are distributed

345 around the globe, since in addition to species found in Australia and North America we  
346 revealed closely related viral RNA metagenomic sequences in the NCBI Sequence Read  
347 Archive (SRX8007769), BioProject accession PRJNA615325 (data not shown). These data  
348 were derived from samples of fish gills collected from Qinghai Lake in Tibet. The largest  
349 encoded protein of these monopartite viruses shows the relationship with RNA polymerases  
350 of benyviruses (Fig. 9), while the capsid protein is distantly related to the tobamovirus CP  
351 (Gibbs et al., 2011; Vlok et al., 2019). Two additional open reading frames (ORFs) code for  
352 an RNA helicase and a protein of unknown function. Importantly, this non-replicative  
353 “accessory” helicase is related to helicases of SF-2 superfamily in contrast to “accessory”  
354 TGB1 helicases belonging to SF-1 (Vlok et al., 2019). It is clear the replicase and tobamo-  
355 like CP genes belong to different lineages of the alphaviruses, orders *Hepelivirales* and  
356 *Martellivirales*, respectively, whereas the “accessory” helicase to replicase of  
357 viruses belonging to order *Amarillovirales* (Vlok et al., 2019).

358 The GBCV genome encodes six polypeptides. Strikingly, the replicase (ORF1) is  
359 more similar to benyvirus-like replicases, whereas coat protein (ORF2) is more closely  
360 related tobamovirus-like CPs (Solovyev and Makarov, 2016) and ORF5 encodes a movement  
361 protein related to the tobamovirus-like MP. Unusual genome organization suggests that  
362 GBCV may represent a recombinant between the viruses from families *Benyviridae* and  
363 *Virgaviridae* (Kwon et al., 2018). This evolutionary episode also suggests a realistic possible  
364 pathway for advanced evolution of TGB, where the horizontal gene transfer of this gene  
365 module from beny-like RNA replicons could occur to ancestral replicons belonging to viruses  
366 belonging to orders *Martellivirales* and *Tymovirales* and initiate the evolution of potex-like  
367 and hordei-like TGBs.

368 Recent studies suggest not only ways of radiation of genome organization for beny-  
369 like replicons but also approximate gene divergence dates. It was shown that the estimates of  
370 gene divergence dates for the RdRp and CP proteins from *Virgaviridae* and *Benyviridae* are  
371 quite different. Generally, wide distribution of tobamo-like CP genes (Solovyev and  
372 Makarov, 2016) in viruses of orders *Hepelivirales* and *Martellivirales* strongly suggests  
373 significant role of horizontal gene transfer in evolutionary radiation of these genes (Shi et al.,  
374 2016). The divergence of the charavirus CP with that of tobamoviruses (family *Virgaviridae*)  
375 was estimated to be 212 million years ago (mya) (Vlok et al., 2019). On the other hand, time  
376 for divergence between charavirus/benyvirus RdRp (order *Hepelivirales*) and virga-like  
377 RdRp genes (order *Martellivirales*) was estimated to be ~900 mya (Vlok et al., 2019). So, it  
378 seems that benyvirus-like replicases started their evolutionary radiations in late Precambrian,

379 *i.e.* perhaps even before the chlorophyte-charophyte split likely occurred 850–1100 million  
380 years ago (Del Cortona et al., 2020; Strassert et al., 2021). In this respect, it is important that  
381 the red algae (Rhodophyta) are most ancient in the kingdom Plantae (Archaeplastida)  
382 (<https://www.algaebase.org/browse/taxonomy/>), and an origin of multicellular red algae is  
383 expected around 1000-1600 mya (Schön et al., 2021; Carlisle et al., 2021; Strassert et al.,  
384 2021). So, the divergence between replication proteins of viruses in orders *Hepelivirales* and  
385 *Martellivirales* could occur in marine red algae species. In support for the proposed role of  
386 Rhodophyta as a host for common ancestors of *Hepelivirales* and *Martellivirales*, it was  
387 found that the both types of virus replicons can be found in modern red algae hosts (Fig. 11).

388

## 389 **EXPERIMENTAL**

390 Virus nucleotide and protein sequences were collected from the NCBI database.  
391 Assembled viral genomes were mainly extracted from NCBI database. The sequence  
392 comparisons were carried out using the BLAST algorithm (BLASTn and BLASTp) at the  
393 National Center for Biotechnology Information (NCBI). Open reading frames (ORFs) were  
394 identified using the NCBI ORF Finder program ([http://www.bioinformatics.org/sms2/orf\\_find.html](http://www.bioinformatics.org/sms2/orf_find.html)). Gene translation and prediction of deduced proteins were performed using  
395 ExPASy (<http://web.expasy.org/translate/>). Conserved motif searches were conducted CDD  
396 (<http://www.ncbi.nlm.nih.gov/Structure/cdd/wrpsb.cgi>) databases. Coiled-coil protein regions  
397 were predicted using Waggawagga software (<https://waggawagga.motorprotein.de/>) (Simm et  
398 al., 2021).

400 To assemble the full-length plant VLRA, transcriptome sequencing data for *D.*  
401 *scoparium* and *C. quitensis* SRA experiments linked to the TSA projects were downloaded  
402 using fastq-dump tool of NCBI SRA Toolkit 2.9.0. (<http://ncbi.github.io/sra-tools/>). Reads  
403 quality was checked with FastQC (<https://www.bioinformatics.babraham.ac.uk/projects/fastqc/>). *De novo* assembly of VLRA coding for TCMB modules was carried out  
404 using SPAdes 3.12.0 (Bankevich et al., 2012) in “RNA mode”.

406 Phylogenetic analysis was performed with “Phylogeny.fr” (a free, simple to use web  
407 service dedicated to reconstructing and analysis of phylogenetic relationships between  
408 molecular sequences) by constructing maximum likelihood phylogenetic trees  
409 ([http://www.phylogeny.fr/simple\\_phylogeny.cgi](http://www.phylogeny.fr/simple_phylogeny.cgi)). Bootstrap percentages received from 1,000  
410 replications were used.

411

412

## 413 **ACKNOWLEDGMENTS**

414 The authors are grateful for the funding received by the Russian Foundation for Basic  
415 Research (grant 20-04-00456).

416

## 417 **AUTHOR CONTRIBUTIONS**

418 SM collected and analyzed the data, authored drafts of the paper;

419 AS authored drafts of the paper, prepared figures, reviewed the final draft.

420

## 421 **CONFLICT OF INTEREST STATEMENT**

422 The authors declare that the research was conducted in the absence of any commercial or  
423 financial relationships that could be construed as a potential conflict of interest.

424

## 425 **DATA AVAILABILITY STATEMENT**

426 The datasets presented in this study can be found in online repositories. The names of the  
427 repository/repositories and accession number(s) mentioned in this paper can be found at:

428 <https://www.ncbi.nlm.nih.gov/>.

429

## 430 **REFERENCES**

431 Bankevich A., Nurk S., Antipov D., Gurevich A.A., Dvorkin M., Kulikov A.S., Lesin V.M.,  
432 Nikolenko S.I., Pham S., Prjibelski A.D., Pyshkin A.V., Sirotkin A.V., Vyahhi N., Tesler G.,  
433 Alekseyev M.A., Pevzner P.A. (2012). SPAdes: a new genome assembly algorithm and its  
434 applications to single-cell sequencing. *J. Comput. Biol.* 19, 455–477.

435

436 Barton D.A., Roovers E. F., Gouil Q., da Fonseca G. C., Reis R. S., Jackson C., Overall R.  
437 L., Fusaro A. F., Waterhouse P/ M. (2017). Live Cell Imaging Reveals the Relocation of  
438 dsRNA Binding Proteins Upon Viral Infection. *Mol. Plant Microbe Interact.* 30, 435-443.  
439 doi: 10.1094/MPMI-02-17-0035-R.

440

441 Bujarski J. J. (2013). Genetic recombination in plant-infecting messenger-sense RNA viruses:  
442 overview and research perspectives. *Front. Plant Sci.* 4, 68. doi: 10.3389/fpls.2013.00068.

443 Cantrill D. J., Poole I. (2013). *The Vegetation of Antarctica through Geological Time*. New  
444 York, NY: Cambridge University Press, 466.

445 Carlisle E. M., Jobbins M., Pankhania V., Cunningham J. A., Donoghue P. C. J. (2021).  
446 Experimental taphonomy of organelles and the fossil record of early eukaryote evolution. *Sci.*  
447 *Adv.* 7, eabe9487. doi: 10.1126/sciadv.abe9487.

448 Chiba S., Hleibieh K., Delbianco A., Klein E., Ratti C., Ziegler-Graff V., Bouzoubaa S.,  
449 Gilmer D. (2013). The benyvirus RNA silencing suppressor is essential for long-distance  
450 movement, requires both zinc-finger and NoLS basic residues but not a nucleolar localization

- 451 for its silencing-suppression activity. *Mol. Plant Microbe Interact.* 26, 168-181. doi:  
452 10.1094/MPMI-06-12-0142-R.
- 453 Del Cortona A., Jackson C. J., Bucchini F., Van Bel M., D'hondt S., Škaloud P., Delwiche C.  
454 F., Knoll A. H., Raven J. A., Verbruggen H., Vandepoele K., De Clerck O., Leliaert F.  
455 (2020). Neoproterozoic origin and multiple transitions to macroscopic growth in green  
456 seaweeds. *Proc. Natl. Acad. Sci. U S A* 117, 2551-2559. doi: 10.1073/pnas.1910060117.
- 457 Dorrington R. A., Jiwaji M., Awando J. A., Bruyn M. M. (2020). Advances in Tetravirus  
458 Research: New Insight Into the Infectious Virus Lifecycle and an Expanding Host Range.  
459 *Curr. Issues Mol. Biol.* 34, 145-162. doi: 10.21775/cimb.034.145.
- 460  
461 Eamens A. L., Kim K. W., Waterhouse P. M. (2012). DRB2, DRB3 and DRB5 function in a  
462 non-canonical microRNA pathway in *Arabidopsis thaliana*. *Plant Signal. Behav.* 7, 1224–  
463 1229. doi: 10.4161/psb.21518.
- 464  
465 Fátyol K., Fekete K. A., Ludman M. (2020). Double-stranded-RNA-binding protein 2  
466 participates in antiviral defense. *J. Virol.* 94, e00017-20. doi: 10.1128/JVI.00017-20.
- 467  
468 Fesenko I., Shabalina S. A., Mamaeva A., Knyazev A., Glushkevich A., Lyapina I.,  
469 Ziganshin R., Kovalchuk S., Kharlampieva D., Lazarev V., Taliansky M., Koonin E. V.  
470 (2021). A vast pool of lineage-specific microproteins encoded by long non-coding RNAs in  
471 plants. *Nucleic Acids Res.* 49, 10328-10346. doi: 10.1093/nar/gkab816.
- 472  
473 Firth A. E., and Brierley, I. (2012). Non-canonical translation in RNA viruses. *J. Gen. Virol.*  
474 93, 1385–1409. doi: 10.1099/vir.0.042499-0.
- 475  
476 Gibbs A. J., Torronen M., Mackenzie A. M., Wood J. T., II, Armstrong J. S., Kondo H., et al.  
477 (2011). The enigmatic genome of *Chara australis* virus. *J. Gen. Virol.* 92, 2679–2690. doi:  
478 10.1099/vir.0.033852-0.
- 479  
480 Gilbert K. B., Holcomb E. E., Allscheid R.L., Carrington, J. C. (2019) Hiding in plain sight:  
481 New virus genomes discovered via a systematic analysis of fungal public transcriptomes.  
482 *PLoS One* 14, e0219207. doi: 10.1371/journal.pone.0219207.
- 483  
484 Han M. H., Goud S., Song L., Fedoroff N. (2004). The *Arabidopsis* double-stranded RNA-  
485 binding protein HYL1 plays a role in microRNA-mediated gene regulation. *Proc. Natl. Acad.*  
486 *Sci. USA* 101, 1093–1098. doi: 10.1073/pnas.0307969100.
- 487  
488 Incarbone M., Clavel M., Monsion B., Kuhn L., Scheer H., Vantard É., Poignavent V.,  
489 Dunoyer P., Genschik P., Ritzenthaler C. (2021). Immunocapture of dsRNA-bound proteins  
490 provides insight into Tobacco rattle virus replication complexes and reveals *Arabidopsis*  
491 DRB2 to be a wide-spectrum antiviral effector. *Plant Cell* 33, 3402-3420. doi:  
492 10.1093/plcell/koab214.
- 493  
494 Kelly A.G., Netzler N. E., White P. A. (2016). Ancient recombination events and the origins  
495 of hepatitis E virus. *BMC Evol. Biol.* 16, 210. doi: 10.1186/s12862-016-0785-y.
- 496

- 497 Koonin E. V., Dolja V. V. (1993). Evolution and taxonomy of positive-strand RNA viruses:  
498 implications of comparative analysis of amino acid sequences. *Crit. Rev. Biochem. Mol. Biol.*  
499 28, 375–430. doi: 10.3109/10409239309078440  
500
- 501 Koonin E. V., Dolja V. V., Krupovic M., Varsani A., Wolf Y. I., Yutin N., Zerbini F. M.,  
502 Kuhn J. H. (2020). Global organization and proposed megataxonomy of the virus world.  
503 *Microbiol. Mol. Biol. Rev.* 84, e00061. doi: 10.1128/MMBR.00061-19.  
504
- 505 Kwon S-J., Choi G-S., Choi B., Seo J-K. (2018). Molecular characterization of an unusual  
506 new plant RNA virus reveals an evolutionary link between two different virus families. *PLoS*  
507 *One* 13, e0206382. <https://doi.org/10.1371/journal.pone.0206382>.
- 508 Lazareva E. A., Lezzhov A. A., Komarova T. V., Morozov S. Y., Heinlein M., Solovyev A.  
509 G. (2017). A novel block of plant virus movement genes. *Mol. Plant Pathol.* 18, 611-624.  
510 doi: 10.1111/mpp.12418.
- 511 Lazareva E. A., Lezzhov A. A., Chergintsev D. A., Golyshev S. A., Dolja V. V., Morozov S.  
512 Y., Heinlein M., Solovyev A. G. (2021). Reticulon-like properties of a plant virus-encoded  
513 movement protein. *New Phytol.* 229, 1052-1066, doi: 10.1111/nph.16905.  
514
- 515 Lehmann A. R. (2005). The role of SMC proteins in the responses to DNA damage. *DNA*  
516 *Repair* (Amst.) 4, 309-314. doi: 10.1016/j.dnarep.2004.07.009.  
517
- 518 Liu S., Valencia-Jiménez A., Darlington M., Vélez A. M., Bonning B. C. (2020). *Diabrotica*  
519 *undecimpunctata virus 2*, a Novel Small RNA Virus Discovered from Southern Corn  
520 Rootworm, *Diabrotica undecimpunctata howardi* Barber (Coleoptera: Chrysomelidae).  
521 *Microbiol. Resour. Announc.* 9, e00380-20. doi: 10.1128/MRA.00380-20.  
522
- 523 Miras M., Miller W. A., Truniger V., Aranda M. A. (2017). Non-canonical Translation in  
524 Plant RNA Viruses. *Front. Plant Sci.* 8, 494. doi: 10.3389/fpls.2017.00494.
- 525 Morozov S. Y., Solovyev A. G. (2003). Triple gene block: modular design of a multi-  
526 functional machine for plant virus movement. *J. Gen. Virol.* 84, 1351–1366. doi:  
527 10.1099/vir.0.18922-0
- 528 Morozov, S. Y., Solovyev, A. G. (2015). Phylogenetic relationship of some ‘accessory’  
529 helicases of plant positive-stranded RNA viruses: toward understanding the evolution of triple  
530 gene block. *Front. Microbiol.* 6, 508. doi: 10.3389/fmicb.2015.00508  
531
- 532 Morozov S. Y., Solovyev A. G. (2020) Small hydrophobic viral proteins involved in  
533 intercellular movement of diverse plant virus genomes. *AIMS Microbiol.* 6, 305-329. doi:  
534 10.3934/microbiol.2020019.  
535
- 536 Niehl A., Liebe S., Varrelmann M., Koenig R. (2020) Benyviruses (*Benyviridae*). *Reference*  
537 *Module in Life Sciences* doi: 10.1016/B978-0-12-809633-8.21298-3.  
538
- 539 Picarelli M.A.S.C., Forgia M., Rivas E. B., Nerva L., Chiapello M., Turina M., Colariccio A.  
540 (2019). Extreme Diversity of Mycoviruses Present in Isolates of *Rhizoctonia solani* AG2-2  
541 LP From *Zoysia japonica* From Brazil. *Front. Cell Infect. Microbiol.* 9, 244. doi:  
542 10.3389/fcimb.2019.00244.

543  
544 Pohlmann T., Baumann S., Haag C., Albrecht M., Feldbrügge M. (2015). A FYVE zinc  
545 finger domain protein specifically links mRNA transport to endosome trafficking. *Elife* 4,  
546 e06041. doi: 10.7554/eLife.06041.  
547  
548 Rodamilans B., Shan H., Pasin F., García J.A. (2018). Plant Viral Proteases: Beyond the Role  
549 of Peptide Cutters. *Front. Plant Sci.* 9, 666. doi: 10.3389/fpls.2018.00666.  
550  
551 Rozanov M. N., Koonin E. V., Gorbalenya A.E. (1992). Conservation of the Putative  
552 Methyltransferase Domain: a Hallmark of the ‘Sindbis-Like’ Supergroup of Positive-Strand  
553 Rna Viruses. *J Gen Virol.* 73, 2129– 2134. doi: 10.1099/0022-1317-73-8-2129.  
554  
555 Saito,M., Kiguchi,T., Kusume,T. and Tamada,T. (1996) Complete nucleotide sequence of the  
556 Japanese isolate S of beet necrotic yellow vein virus RNA and comparison with European  
557 isolates. *Arch. Virol.* 141, 2163-2175. doi: 10.1007/BF01718223.  
558  
559 Schön M. E., Zlatogursky V. V., Singh R. P., Poirier C., Wilken S., Mathur V., Strassert J. F.  
560 H., Pinhassi J., Worden A. Z., Keeling P. J., Ettema T. J. G., Wideman J. G., Burki F. (2021).  
561 Single cell genomics reveals plastid-lacking Picozoa are close relatives of red algae. *Nat.*  
562 *Commun.* 12, 6651. doi: 10.1038/s41467-021-26918-0.  
563  
564 Shi M., Lin X-D., Tian J-H., et al. (2016). Redefining the invertebrate RNA virosphere.  
565 *Nature* 540, 539–543. doi: 10.1038/nature20167.  
566  
567 Simm D., Hatje K., Waack S., Kollmar M. (2021) Critical assessment of coiled-coil  
568 predictions based on protein structure data. *Sci. Rep.* 11, 12439. doi: 10.1038/s41598-021-  
569 91886-w.  
570  
571 Solovyev A.G., Makarov V. V. (2016). Helical capsids of plant viruses: architecture with  
572 structural lability. *J. Gen. Virol.* 97, 1739-1754. doi: 10.1099/jgv.0.000524.  
573  
574 Solovyev A. G., Morozov, S. Y. (2017) Non-replicative Integral Membrane Proteins Encoded  
575 by Plant Alpha-Like Viruses: Emergence of Diverse Orphan ORFs and Movement Protein  
576 Genes. *Front. Plant. Sci.* 8, 1820. doi: 10.3389/fpls.2017.01820.  
577  
578 Strassert J. F. H., Irisarri I., Williams T. A., Burki F. (2021). A molecular timescale for  
579 eukaryote evolution with implications for the origin of red algal-derived plastids. *Nat.*  
580 *Commun.* 12, 1879. doi: 10.1038/s41467-021-22044-z.  
581  
582 Tilsner, J., Linnik, O., Louveaux, M., Roberts, I. M., Chapman, S. N., and Oparka, K. J.  
583 (2013). Replication and trafficking of a plant virus are coupled at the entrances of  
584 plasmodesmata. *J. Cell Biol.* 201, 981–995. doi: 10.1083/jcb.201304003  
585  
586 Vakirlis N., Acar O., Hsu B., Castilho Coelho N., Van Oss S. B., Wacholder A., Medetgul-  
587 Ernär K., Bowman R.W. 2nd, Hines C. P., Iannotta J., Parikh S. B., McLysaght A., Camacho  
588 C. J., O'Donnell A. F., Ideker T., Carvunis A. R. (2020). De novo emergence of adaptive  
589 membrane proteins from thymine-rich genomic sequences. *Nat. Commun.* 11, 781. doi:  
590 10.1038/s41467-020-14500-z.  
591



592 Verchot-Lubicz, J., Torrance, L., Solovyev, A.G., Morozov, S.Y., Jackson, A.O., and Gilmer,  
593 D. (2010). Varied movement strategies employed by triple gene block-encoding viruses. *Mol.*  
594 *Plant-Microbe Interact.* 23, 1231-1247. doi: 10.1094/MPMI-04-10-0086.

595

596 Vlok, M., Gibbs, A. J., and Suttle, C. A. (2019). Metagenomes of a Freshwater Charavirus  
597 from British Columbia Provide a Window into Ancient Lineages of Viruses. *Viruses* 11, 299.  
598 doi: 10.3390/v11030299.

599

600 Zhu J. Z., Zhu H. J., Gao B. D., Zhou Q., Zhong J. (2018) Diverse, Novel Mycoviruses From  
601 the Virome of a Hypovirulent *Sclerotium rolfsii* Strain. *Front. Plant Sci.* 9, 1738. doi:  
602 10.3389/fpls.2018.01738.

603

604

605

606

607

608

609

610

611

612

613

614

615

616

617

618

619

620

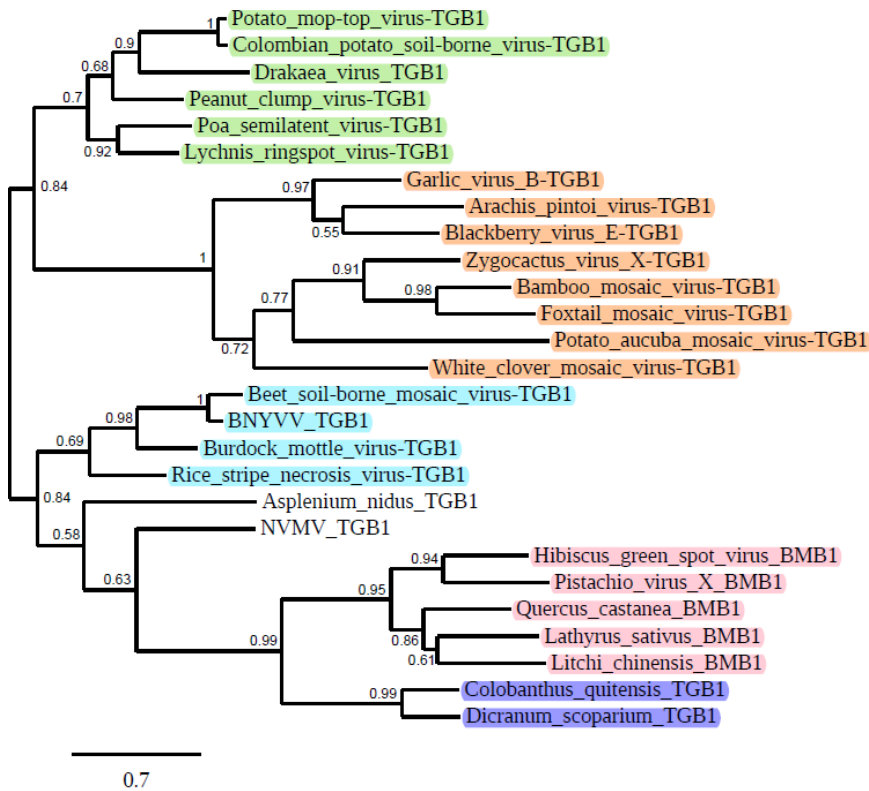
621

622

623

624

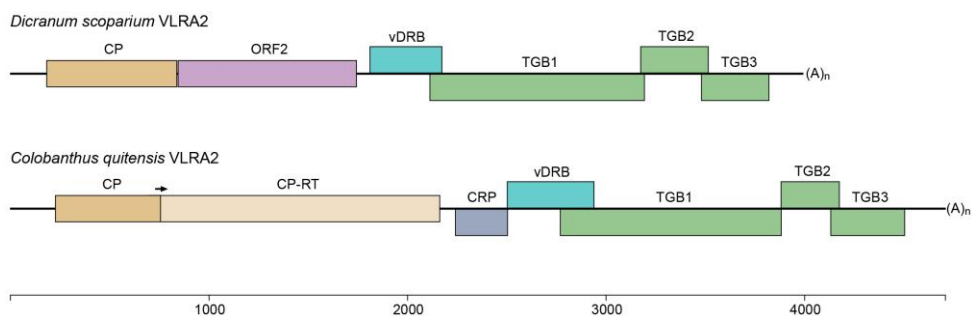
625 **FIGURES AND LEGENDS**



626

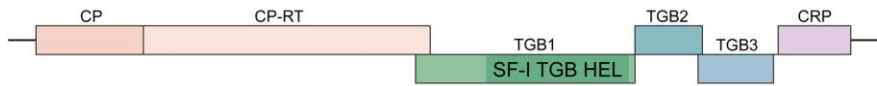
627 **Fig. 1.** Phylogenetic analysis of the helicase domains derived from the aligned deduced  
 628 amino acid sequences of the proteins encoded by TGBs and BMBs. The phylogenetic  
 629 unrooted tree was constructed using the maximum likelihood method based on the amino  
 630 acid sequence alignments ([http://www.phylogeny.fr/simple\\_phylogeny.cgi](http://www.phylogeny.fr/simple_phylogeny.cgi)). The bootstrap  
 631 values obtained with 1000 replicates are indicated on the branches, and branch lengths  
 632 correspond to the branch line's genetic distances. The genetic distance is shown by the scale  
 633 bar at the lower left. BNYVV – beet necrotic yellow vein virus; NVMV – Nicotiana velutina  
 634 mosaic virus. Hordei-like TGB1 helicases are in green, potex-like helicases – in brown,  
 635 benyvirus TGB1 helicases are in blue, BMB1 helicases found two viruses and three VLRA  
 636 (*Q. castanea*, *L. sativus* and *L. chinensis*) are in pink, TCMB helicases found in the  
 637 corresponding VLRA (*C. quitensis* and *D. scoparium*) are in dark blue.

638 **A**



639

640 **B**

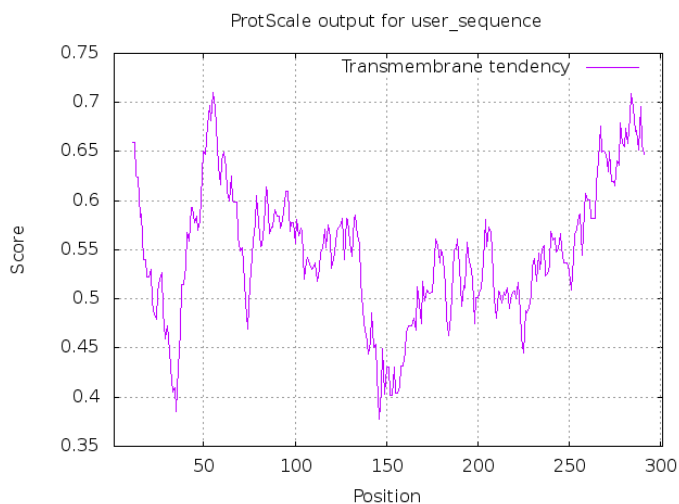


641

642 **Fig. 2.** Comparison of gene organization of RNA2 genomic components encoding  
 643 multicomponent cell-to-cell transport systems in *D.scoparium* and *C.quitensis* VLRA (A)  
 644 and Beet necrotic yellow vein virus (B). Genes are shown as boxes with the names of the  
 645 encoded proteins. Genes of proteins potentially involved in cell-to-cell movement (TGB and  
 646 vDRB) are shown in green, dark green, light green and blue-green. Genes encoding small  
 647 hydrophobic proteins are shown in blue. Replicative genes are shown in yellow. Arrows  
 648 indicate read-through codons in CP-RT proteins. CRP – cysteine-rich protein, CP-RT – coat  
 649 protein read-through protein.

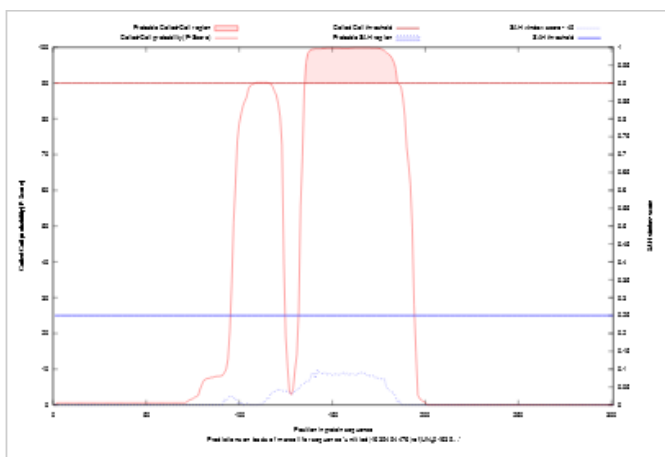
650

651 **A**



652

653 **B**



654

655 **Fig. 3. (A)** Prediction of hydrophobic membrane-bound regions ([https://web.expasy.org/](https://web.expasy.org/protscale/)  
 656 [protscale/](https://web.expasy.org/protscale/)) and **(B)** coiled-coil segments (above red cut-off line) (<https://waggawagga.motorprotein.de/>)  
 657 in ORF2 protein of Ds-VLRA2.

658  
 659

```

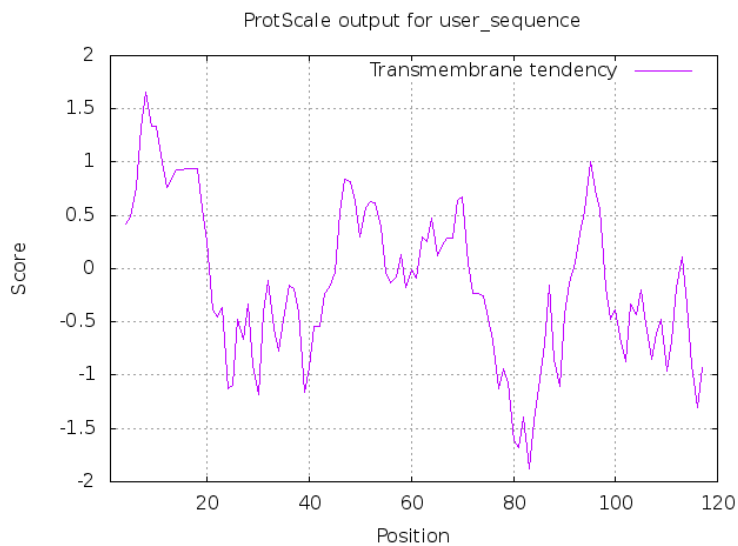
660 DsORF3-RNLLQETLQAKGGLLPVYFTYSYLAADGGICWGSVSAFGIT-ERALNYKMKVAEC
661 CqORF4-KSALQVQTPRAYEDLPITYTSRRVGNLWFSRVDCYLGSAYGVA-----GRKKVADC
662 AtDRB4-KNLLQETIAQKESLLPFYATATSGPSHAPTFT-STVEFAGKV-FSGEEAKTKKLAEM
663 AtHYL1-KSRLQETYAQKYKLPVYEVIVKEGSPSHKSLFQ-STVILDGVRYNLSLPGFFNRKAAEQ
664 AtDRB5-KNLLQETAHRAGLDLPVYTSVRSKSGSHPGFGFS-CTVELAGMT-FTGESAKTKKQAEK
665 CpDRBL-KNLLQETAQRAGVSLPVYATTRSGLPGHLPVFT-CTVEVASMT-FNGEAAKTKKQAEK
666 PpDRB2-KNLLQETAQRAGVSLPVYATTRSGLPGHLPVFT-CTVEVASMT-FSGEAAKTKKQAEA
667 SmDRBL-KNLLQETAQRAGVPLPIYTTVRSGLPGHLPVFT-CTVGVGGMI-FTGEAAKTKKQAEA
668 MpDRBL-KNLLQETAQRAGVSLPVYTTTRSGLPGHLPVFT-CQVELAGMK-FDGEAAKTKKQAEK
669 CbDRBL-KNLLQETSQRAGVSLPVYHAMRMGPDHQPVYS-ASVEVAGMR-FYGCQAKTKKQAEK
670 NmDRBL-KNLLQETSQRAGVPLPVYHAMRMGPDHQPVYS-ASVEVAGMR-FYGCQAKTKKQAEK
671 SpDRBL-KNLLQETPQRAGIPLPIYITTRMGPDHLPVYS-SSVEMAGMR-FYGESAKTKKQAEK
672
    
```

673 **Fig. 4.** Multiple sequence alignment of the dsRNA-binding centers of proteins HYL1, DRB4  
 674 and DRB5 from *A. thaliana* with vDRB proteins of *D. scoparium* (DsORF3) and *C.*  
 675 *quitensis* (CqORF4) as well as DRB-like proteins of moss *Ceratodon purpureus* (CpDRBL -  
 676 accession KAG0625911), moss *Physcomitrium patens* (PpDRB2 - XP\_024393530),  
 677 lycophyte *Selaginella moellendorffii* (SmDRBL - EFJ14280), liverwort *Marchantia*  
 678 *polymorpha* (MpDRBL - PTQ26790), charophyte algae *Chara braunii* (CbDRBL -  
 679 GGXX01036972), charophyte algae *Nitella mirabilis* (NmDRBL - JV799478), charophyte  
 680 algae *Spirogyra pratensis* (SpDRBL - GFWN01008525).

681

682

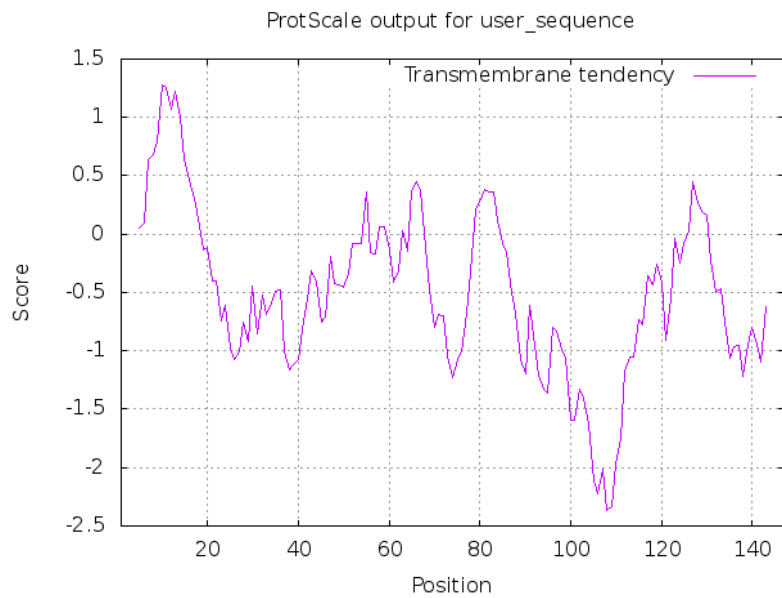
683 ***D. scoparium***



684

685

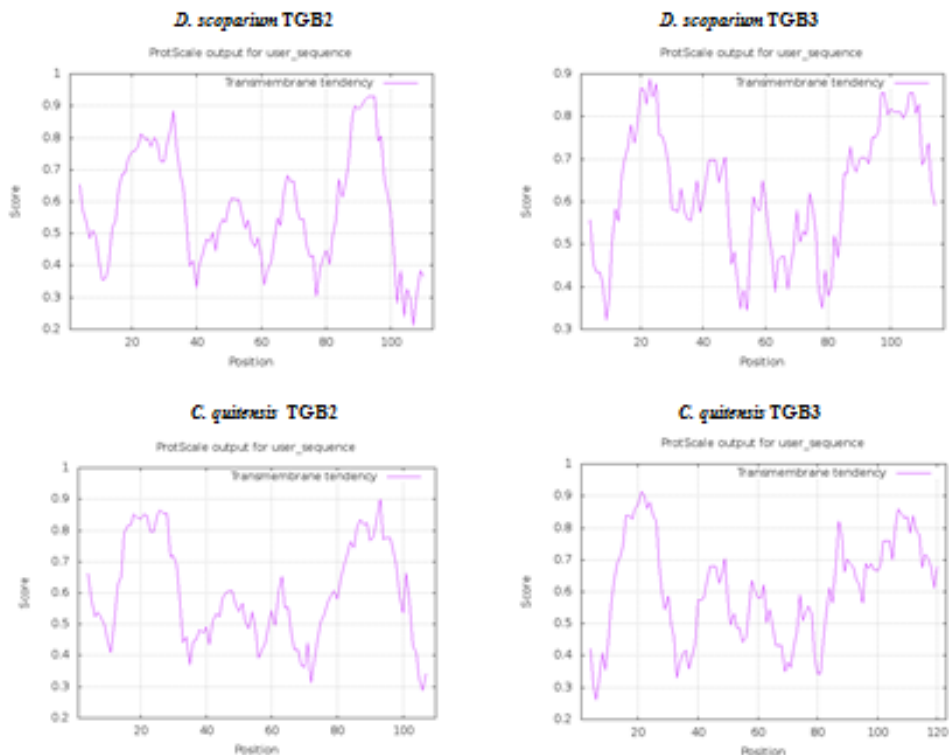
686 *C. quitensis*



687

688 **Fig. 5.** Prediction of hydrophobic membrane-bound regions (<https://web.expasy.org/protscale/>) in vDRB proteins of *D. scoparium* (DsORF3) and *C. quitensis* (CqORF4).

689 Membrane-bound protein segments are above 0.8 cutoff line.



691

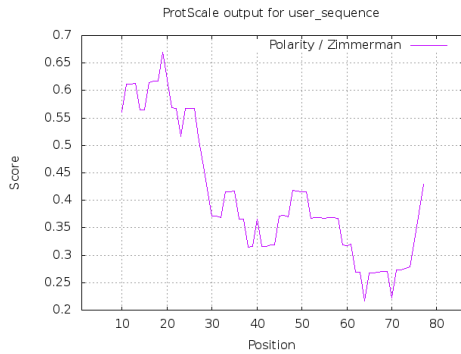
692 **Fig. 6.** Prediction of hydrophobic membrane-bound regions (<https://web.expasy.org/protscale/>) in TGB-like proteins of *D. scoparium* and *C. quitensis* VLRA.

693

694 **A**

695 MGDHVVVLLIEKREAKLEKEENARNLKRFRIVEVEKGVWYQLEEGECFCSSSIHKHCAKCGEPTDGYCVMCSCELRARQAYRTNERRK  
 696

697 **B**



698

699 **Fig. 7. (A)** Amino acid sequence of an ORF3 protein encoded by Cq-VLRA2. Positively  
 700 charged residues are shown in red, negatively charged – in blue, cysteines – in yellow.

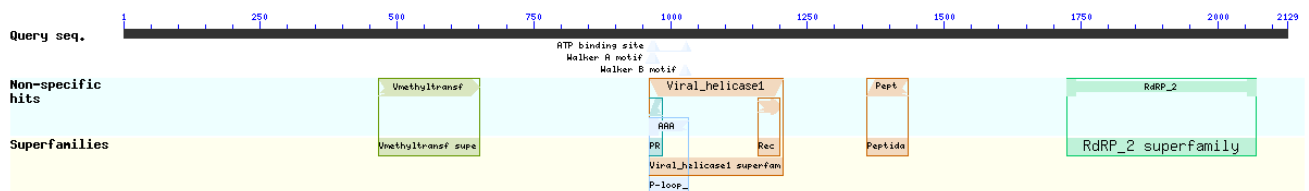
701 Putative zinc finger motif-containing module is underlined. **(B)** Polarity plot of ORF3 protein  
 702 (<https://web.expasy.org/protscale/>).

703

704

705

706 **A**



707

708

709

710 **B**

711

712 **RNA1**

713 CTATTGAGCGACAACAGTATCCGAGCT-AGACTCGTAAAGGCTCTGAACTGGCTCTTTTAGCAAGTATGATTCCCGAAATG-AAAGGCTGTTATTTATTGCTGCTCTGACATAGAGTTT (A) n

714 CTATTGGA-TGA-GACAGTATCCGAGCAAGACTCGTAAAGGCTCTGAACTCCTG---AAACCGAATGCCTTTCCTGTATGAAAAGGGAAC--GATTATTGCAACTCTGTAGATAGAGTTT (A) n

715 **RNA2**

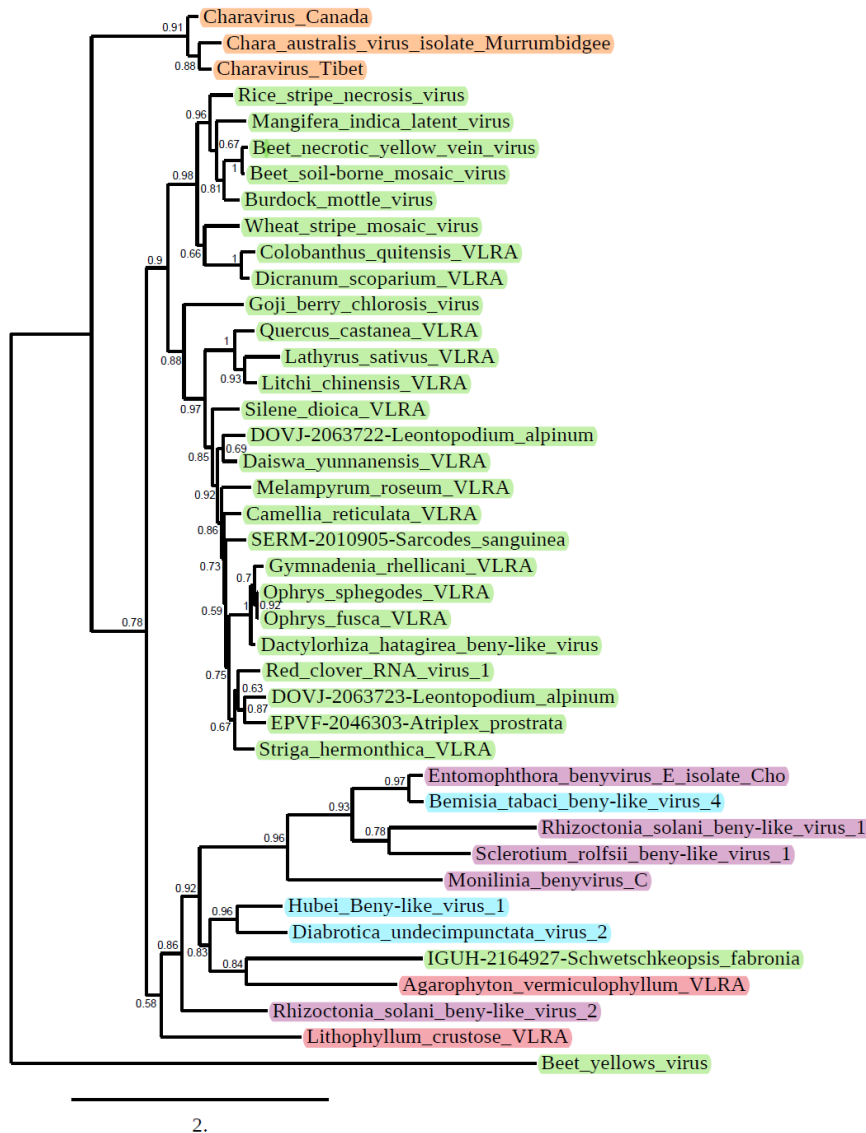
716

717 **Fig. 8. (A)** The predicted organization of ORF1 protein of Ds-VLRA1 (NCBI format)

718 containing four conserved domains: a viral methyltransferase domain (Vmethyltransf, amino  
 719 acid positions 440–625); a viral helicase 1 domain (amino acid positions 939–1179); papain-  
 720 like proteinase domain (Pept, positions 1333–1408), and RdRp core motif (RdRP 2

721 superfamily, amino acid positions 1698–2045). **(B)** Nucleotide sequence alignment of the 3'-

722 terminal regions preceding poly(A) in the predicted VLRA RNAs 1 and 2 from *Dicranum*  
723 *scoparium*. Highly conserved RNA blocks are highlighted by yellow and green background.

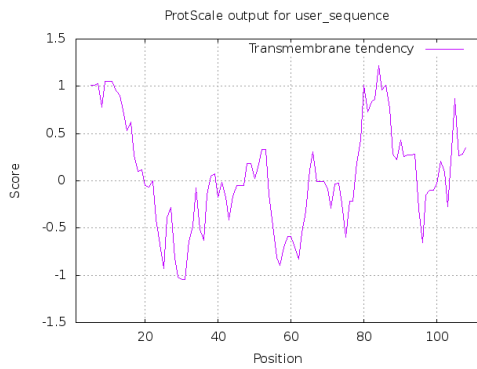


724  
725 **Fig. 9.** Phylogenetic analysis of the conserved motifs of RdRp derived from the aligned  
726 deduced amino acid sequences of beny-like viruses and selected VLRA. The phylogenetic  
727 tree was constructed using the maximum likelihood method at Phylogeny.fr. The beet  
728 yellows closterovirus RdRp was used as outgroup. The bootstrap values obtained with 1000  
729 replicates are indicated on the branches, and branch lengths correspond to the branch line's  
730 genetic distances. The genetic distance is shown by the scale bar at the lower left.  
731 Charaviruses are shown in brown, plant viruses are in green, fungal viruses are in pink,  
732 arthropod viruses are in blue, red algae viruses are in rose.

733

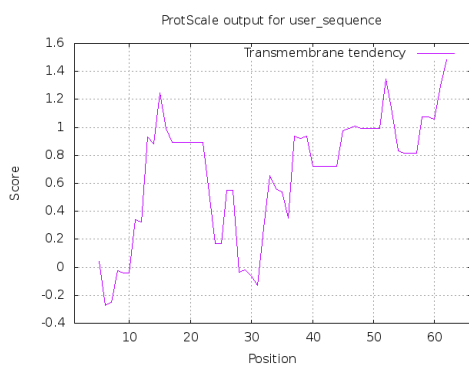
734

735 **A**



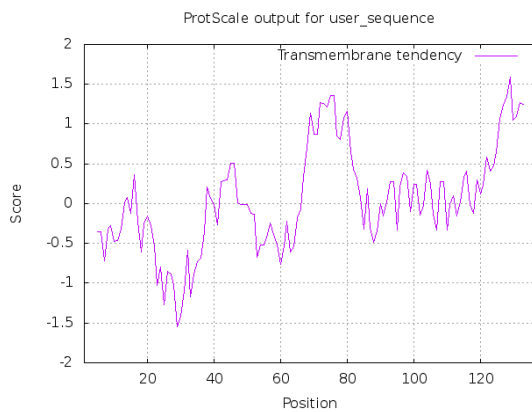
736

737 **B**



738

739 **C**



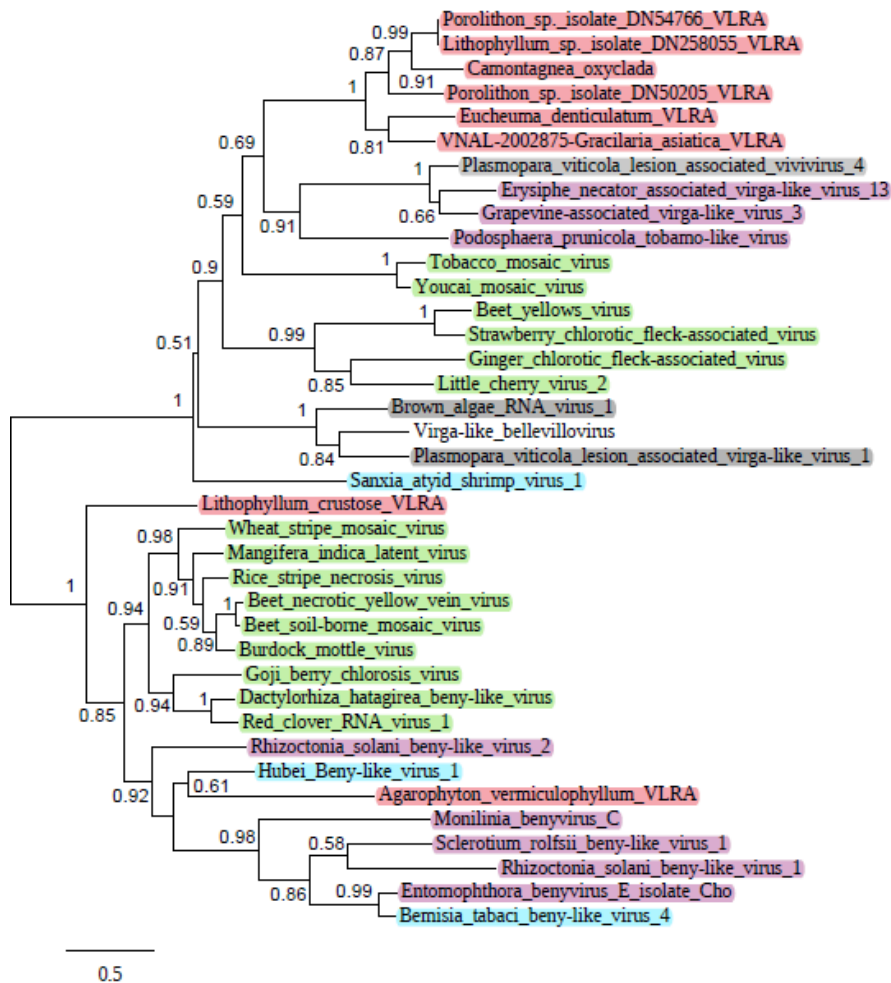
740

741 **Fig. 10.** Prediction of hydrophobic membrane-bound regions ([https://web.expasy.org/](https://web.expasy.org/protscale/)  
742 protscale/) in p2 (**A**) and p3 (**B**) “orphan” proteins of Red clover RNA virus 1 (accession  
743 MG596242) as well as ORF2 protein (**C**) of Dactylorhiza hatagirea beny-like virus (accession  
744 BK013327). Membrane-bound protein segments are above 0.8 cutoff line.

745

746





747

0.5

748 **Fig. 11.** Phylogenetic analysis of the conserved motifs of RdRp derived from the aligned  
 749 deduced amino acid sequences of selected beny-like replicative proteins (bottom branch),  
 750 virga-like replicative proteins (upper branch) and red algae VLRA. The unrooted  
 751 phylogenetic tree was constructed using the maximum likelihood method at Phylogeny.fr.  
 752 The bootstrap values obtained with 1000 replicates are indicated on the branches, and branch  
 753 lengths correspond to the branch line's genetic distances. The genetic distance is shown by  
 754 the scale bar at the lower left. Viruses of Stramenopiles are shown as shaded, plant viruses  
 755 are in green, fungal viruses are in pink, arthropod viruses are in blue, red algae viruses are in  
 756 rose.

757

758

759

760

761